degradation of p53 protein. In response to DNA damage, p53 is induced, accumulated and finally degraded after the removal of the DNA damage. Our results suggest that cyclin G1 is involved in the accumulation and degradation of p53 protein through its ability to associate, respectively, with MDM2 complexes containing either ARF or PP2A.

Many cyclins have been shown to associate with and regulate the cyclin dependent kinases (cdks). We previously reported the association of cyclin G1 with cdk5, a member of the cdk family, and with GAK, a protein kinase with a low similarity to cdk (Kanaoka *et al.* 1997; Kimura *et al.* 1997). Unexpectedly, we found that cyclin G1 could not regulate the activities of these kinases (Kimura *et al.* 1997). Thus, the authentic cdk partner of cyclin G1 has yet to be identified. In this report, we show that PP2A associates with the cyclin G1/MDM2 complex during the late post-irradiation period. This result suggests that cyclin G1 promotes PP2A to associate with MDM2, and that the phosphatase activity of PP2A regulates the activity of MDM2 to ubiquitinate p53. Cyclin G1 may regulate the phosphatase activity of PP2A or play a role as a component of the PP2A-phosphatase complex. It was very recently reported that cyclin G1 actually regulates the phosphatase activity of PP2A and promotes the dephosphorylation of MDM2 (Okamoto *et al.* 2002). These authors also showed that the level of p53 was higher in cyclin $G1^{-/-}$ cells without any DNA damage; however, they did not describe how the cyclin G1 affected p53 levels after DNA damage. We report here that p53 level in cyclin $G1^{-/-}$ cells is higher than that in wild-type cells without DNA damage and at 48 h after DNA damage (Fig. 5). We further show here that p53 level in cyclin $G1^{-/-}$ cells is decreased between 6 h and 24 h following DNA damage. These results suggest that the effect of cyclin G1 on p53 levels depends upon the cellular situation and experimental conditions. We further report here that cyclin G2, which is known to be induced in response to DNA damage in a p53-independent manner (Bates *et al.* 1996), also interacts with MDM2 and PP2A (Fig. 6C). The result suggests that cyclin G2 may complement the function of cyclin G1 in cyclin $G1^{-/-}$ cells. Generation of cyclin G1/cyclin G2 double knock out mice may help to understand the functional interactions between these closely related genes.

Experimental procedures

Cell culture

Primary MEFs were obtained from mouse embryos using established procedures (Robertson 1987). MEFs were cultured at 37 °C in a 5% CO_2 atmosphere in Dulbecco's modified Eagle's medium (DMEM) supplemented with 10% heat-inactivated foetal calf serum (FCS), 2 mM L-glutamine, 0.1 mM sodium pyruvate, 100 U/mL penicillin G, 100 μg/mL streptomycin sulphate and 50 μM 2-mercaptoethanol. 293T cells were maintained in 5% CO_2 at 37 °C in DMEM supplemented with 5% FCS, penicillin (100 U/mL) and streptomycin (100 μg/mL).

Irradiation and transfection of cells

Cells were subjected to a 10-Gy dose of γ radiation in a Gammacell 40 Exactor Research Irradiator (MDS Nordion, Ontario, Canada) with a ^{137}Cs source at a rate of 1.142 Gy/min. The UV irradiation of MEFs was performed on cells that had the culture medium and plate cover removed. Induction of p53 in these cells was achieved by irradiating them with a germinal lamp at a rate of 0.22 $J/m^2/s$. In order to induce over-expression of cyclin G1 and cyclin G2, pBabe-puro-cyclin G1 and/or pBabe-puro-cyclin G2 were constructed and retrovirus-mediated gene transfer was carried out as previously described (Morgenstern & Land 1990; Pear *et al.* 1993). For the lipofection assays, FLAG-cyclin G1, Myc-ARF and GFP-MDM2 were cloned into the pAP3neo, pCDNA3 and pEGFP-3B vectors, respectively. Lipofections were performed as previously described (Kimura *et al.* 2001).

Immunoprecipitation and Western blot analysis

Immunoprecipitation was performed essentially as previously described (Kanaoka *et al.* 1997). Briefly, cells were collected and lysed in lysis buffer (50 mM Tris-HCl [pH 7.5], 250 mM NaCl, 0.1% Nonidet P-40) supplemented with protease inhibitors (2 μg/mL Aprotinin, 2 μg/mL of Leupeptin, 1 μg/mL Pepstatin A, 50 μg/mL PMSF, 1 mM EGTA). After clarifying the extract by centrifugation at 10 000 *g* for 5 min, aliquots of the supernatant were immunoprecipitated by the use of protein A-Sepharose alone. The clarified lysates were subsequently immunoprecipitated using the relevant antibodies. Equal quantities of fresh or immunoprecipitated cell extract were then adsorbed to protein A-Sepharose, pelleted and subjected to 10% SDS–polyacrylamide gel electrophoresis (SDS-PAGE). For Western blotting, total cellular proteins and immunoprecipitates resolved on gels were transferred to nitrocellulose filters and probed with the relevant antibodies. Immunoreactive protein bands were visualized using Renaissense™ chemiluminescence reagents (DuPont NEN).

Antibodies

Anti-cyclin G1 and anti-cyclin G2 polyclonal antibodies were raised as described elsewhere (Kanaoka *et al.* 1997; Kimura *et al.* 2001). Anti-MDM2 SMP14 (Santa Cruz), anti-Myc Ab-1 (Oncogene Science), anti-FLAG M2 (Eastman Kodak), anti-tubulin (MBL) monoclonal antibodies, anti-p19ARF G19 (Santa Cruz), anti-p53 FL-393 (Santa Cruz) polyclonal antibodies, and secondary antibodies against mouse, rabbit and goat IgG (CAPPEL) were purchased from the specified companies. Anti-GFP polyclonal antibody was a gift from Dr K. Tamai (MBL Co. Ltd, Nagoya).

Pulldown assay

DNA fragments of cyclin G1, MDM2 and ARF with a *AscI* or *NotI* restriction site at their 5′ or 3′ end were inserted into pGEX-8T and pMAC-3B to produce GST- and FLAG-fusion proteins in *E. coli*, respectively. In order to purify the GST-fusion protein, 200 mL of *E. coli* cells expressing the GST-fusion protein were grown to mid-log phase at 20 °C. Cells were collected, washed with 10 mL of ice-cold PBS, resuspended in 2 mL of IP buffer (50 mM Tris-Cl, pH 8.0/0.2 M NaCl/0.1% Triton X-100) and lysed by sonication. Triton X-100 was added to 1%, and the cell debris was then removed by centrifugation. Supernatants were diluted with ice-cold IP buffer to give a final concentration of 10 mg/mL protein, mixed with 100 μL of glutathion-Sepharose beads per mL and incubated at 4 °C overnight. Beads were pelleted by centrifugation and washed five times with 500 μL of IP buffer. One-fourth of the bead volume was added to 2 mg of cell extract containing FLAG-fusion protein. The lysates prepared from *E. coli* expressing FLAG-fusion proteins were mixed with each other as indicated in Fig. 3. The lysates were mixed with the beads by overnight rotation at 4 °C, and then the proteins bound to the beads were recovered and washed three times in one volume of IP buffer. Final pellets were subjected to SDS-PAGE and Western blotting with anti-GST or anti-FLAG antibody.

Acknowledgements

We thank Ms K. Yamauchi for technical assistance, Dr N. Yoshioka for the retroviral vector, pBabe-Puro, Dr M. Yutsudo for the 293T cells, Dr K. Tamai for the anti-GFP antibody, and Dr K. Nabeshima for helpful discussions. This work was supported by grants from the Ministry of Education, Culture, Sports, Science and Technology of Japan, and grants from the Osaka Cancer Society, Uehara Foundation, Yasuda Medical Research Foundation, Osaka Cancer Research Foundation, and the Japanese Foundation for Multidisciplinary Treatment of Cancer.

References

Barak, Y., Juven. T., Haffner, R. & Oren, M. (1993) mdm2 expression is induced by wild type p53 activity. *EMBO J.* **12**, 461–468.

Bates, S., Rowan, S. & Vousden, K.H. (1996) Characterisation of human cyclin G1 and G2: DNA damage inducible genes. *Oncogene* **13**, 1103–1109.

Chehab, N.H., Malikzay, A., Appel, M. & Halazonetis, T.D. (2000) Chk2/hCds1 functions as a DNA damage checkpoint in G(1) by stabilizing p53. *Genes Dev.* **14**, 278–288.

Chehab, N.H., Malikzay, A., Stavridi, E.S. & Halazonetis, T.D. (1999) Phosphorylation of Ser-20 mediates stabilization of human p53 in response to DNA damage. *Proc. Natl. Acad. Sci. USA* **96**, 13777–13782.

Dameron, K.M., Volpert, O.V., Tainsky, M.A. & Bouck, N. (1994) Control of angiogenesis in fibroblasts by p53 regulation of thrombospondin-1. *Science* **265**, 1582–1584.

Donehower, L.A., Harvey, M., Slagle, B.L., *et al.* (1992) Mice deficient for p53 are developmentally normal but susceptible to spontaneous tumours. *Nature* **356**, 215–221.

El-Deiry, W.S. (1998) p21/p53, cellular growth control and genomic integrity. *Curr. Top. Microbiol. Immunol.* **227**, 121–137.

Freedman, D.A. & Levine, A.J. (1998) Nuclear export is required for degradation of endogenous p53 by mdm2 and human papillomavirus E6. *Mol. Cell. Biol.* **18**, 7288–7293.

Hermeking, H., Lengauer, C., Polyak, K., *et al.* (1997) 14-3-3 sigma is a p53-regulated inhibitor of G2/M progression. *Mol. Cell* **1**, 3–11.

Hirao, A., Kong, Y.Y., Matsuoka, S., *et al.* (2000) DNA damage-induced activation of p53 by the checkpoint kinase Chk2. *Science* **287**, 1824–1827.

Honda, R., Tanaka, H. & Yasuda, H. (1997) Oncoprotein MDM2 is a ubiquitin ligese E3 for tumor suppressor p53. *FEBS Lett.* **420**, 25–27.

Honda, R. & Yasuda, H. (1999) Association of p19ARF with Mdm2 inhibits ubiquitin ligase activity of Mdm2 for tumor suppressor p53. *EMBO J.* **18**, 22–27.

Horne, M.C., Donaldson, K.L., Goolsby, G.L., *et al.* (1997) Cyclin G2 is up-regulated during growth inhibition and B cell antigen receptor-mediated cell cycle arrest. *J. Biol. Chem.* **272**, 12650–12661.

Horne, M.C., Goolsby, G.L., Donaldson, K.L., Tran, D., Neubauer, M. & Wahl, A.F. (1996) Cyclin G1 and cyclin G2 comprise a new family of cyclins with contrasting tissue-specific and cell cycle-regulated expression. *J. Biol. Chem.* **271**, 6050–6061.

Hunt, T. (1991) Cyclins and their partners: from a simple idea to complicated reality. *Semin Cell Biol.* **2**, 213–222.

Kamijo, T., Weber, J.D., Zambetti, G., Zindy, F., Roussel, M.F. & Sherr, C.J. (1998) Functional and physical interactions of the ARF tumor suppressor with p53 and Mdm2. *Proc. Natl. Acad. Sci. USA* **95**, 8292–8297.

Kanaoka, Y., Kimura, S.H., Okazaki, Ikeda, M. & Nojima, H. (1997) GAK: a cyclin G associated kinase contains a tensin/auxilin-like domain. *FEBS Lett.* **402**, 73–80.

Kimura, S.H., Ikawa, M., Ito, A., Okabe, M. & Nojima, H. (2001) Cyclin G1 is required for the recover of damages and the cell proliferation after cellular stresses. *Oncogene* **20**, 3290–3300.

Kimura, S.H., Tsuruga, H., Yabuta, N., Endo, Y. & Nojima, H. (1997) Structure, expression, and chromosomal localization of human GAK. *Genomics* **44**, 179–187.

Maki, C.G., Huibregtse, J.M. & Howley, P.M. (1996) In vivo ubiquitination and proteasome-mediated degradation of p53. *Cancer Res.* **56**, 2649–2654.

Miyashita, T. & Reed, J.C. (1995) Tumor suppressor p53 is a direct transcriptional activator of the human bax gene. *Cell* **80**, 293–299.

Morgenstern, J.P. & Land, H. (1990) s gene transfer: high titre retroviral vectors with multiple drug selection markers and a complementary helper-free packaging cell line. *Nucl. Acids Res.* **18**, 3587–3596.

Nakamura, T., Sanokawa, R., Sasaki, Y.F., Ayusawa, D., Oishi, M. & Mori, M. (1995) Cyclin I: a new cyclin encoded by a gene isolated from human brain. *Exp. Cell Res.* **221**, 534–542.

Nugent, J.H., Alfa, C.E., Young, T. & Hyams, J.S. (1991) Conserved structural motifs in cyclins identified by sequence analysis. *J. Cell Sci.* **99**, 669–674.

Okamoto, K. & Beach, D. (1994) Cyclin G is a transcriptional target of the p53 tumor suppressor protein. *EMBO J.* **13**, 4816–4822.

Okamoto, K., Kamibayashi, C., Serrano, M., Prives, C., Mumby, M.C. & Beach, D. (1996) p53-dependent association between cyclin G and the B′ subunit of protein phosphatase 2A. *Mol. Cell. Biol.* **16**, 6593–6602.

Okamoto, K., Li, H., Jensen, M.R., *et al.* (2002) Cyclin G recruits PP2A to dephosphorylate Mdm2. *Mol. Cell* **9**, 761–771.

Okamoto, K. & Prives, C. (1999) A role of cyclin G in the process of apoptosis. *Oncogene* **18**, 4606–4615.

Pear, W.S., Nolan, G.P., Scott, M.L., *et al.* (1993) Production of high-titer helper-free retroviruses by transient transfection. *Proc. Natl. Acad. Sci. USA* **90**, 8392–8396.

Pines, J. (1991) Cyclins: wheels within wheels. *Cell Growth Differ.* **2**, 305–310.

Pomerantz, J., Schreiber-Agus, N., Liegeois, N.J., *et al.* (1998) The Ink4a tumor suppressor gene product, p19Arf, interacts with MDM2 and neutralizes MDM2's inhibition of p53. *Cell* **92**, 713–723.

Reimer, C.L., Borras, A.M., Kurdistani, S.K., *et al.* (1999) Altered regulation of cyclin G in human breast cancer and its specific localization at replication foci in response to DNA damage in $p53^{+/+}$ cells. *J. Biol. Chem.* **274**, 11022–11029.

Robertson, E.J. (1987) *Teratocarcinoma and Embryonic Stem Cells: a Practical Approach*, pp. 77–78. Oxford: IRL Press.

Roth, J., Dobbelstein, M., Freedman, D., Shenk, T. & Levine, A.J. (1998) Nucleocytoplasmic shuttling of the hdm2 oncoprotein regulates the levels of the p53 protein via a pathway used by the human immunodeficiency virus rev protein. *EMBO J.* **17**, 554–564.

Shieh, S.Y., Ahn, J., Tamai, K., Taya, Y. & Prives, C. (2000) The human homologs of checkpoint kinases Chk1 and Cds1 (Chk2) phosphorylate p53 at multiple DNA damage-inducible sites. *Genes Dev.* **14**, 289–300.

Shieh, S.Y., Ikeda, M., Taya, Y. & Prives, C. (1997) DNA damage-induced phosphorylation of p53 alleviates inhibition by MDM2. *Cell* **91**, 325–334.

Shieh, S.Y., Taya, Y. & Prives, C. (1999) DNA damage-inducible phosphorylation of p53 at N-terminal sites including a novel site, Ser20, requires tetramerization. *EMBO J.* **18**, 1815–1823.

Smith, M.L., Chen, I.-T., Zhan, Q., *et al.* (1994) Interaction of the p53-regulated protein Gadd45 with proliferating cell nuclear antigen. *Science* **266**, 1376–1379.

Stott, F.J., Bates, S., James, M.C., *et al.* (1998) The alternative product from the human CDKN2A locus, p14 (ARF), participates in a regulatory feedback loop with p53 and MDM2. *EMBO J.* **17**, 5001–5014.

Tamura, K., Kanaoka, Y., Jinno, S., *et al.* (1993) Cyclin G: a new mammalian cyclin with homology to fission yeast Cig1. *Oncogene* **8**, 2113–2118.

Tao, W. & Levine, A.J. (1999) Nucleocytoplasmic shuttling of oncoprotein Hdm2 is required for Hdm2-mediated degradation of p53. *Proc. Natl. Acad. Sci. USA* **96**, 6937–6941.

Tibbetts, R.S., Brumbaugh, K.M., Williams, J.M., *et al.* (1999) A role for ATR in the DNA damage-induced phosphorylation of p53. *Genes Dev.* **13**, 152–157.

Unger, T., Juven-Gershon, T., Moallem, E., *et al.* (1999) Critical role for Ser20 of human p53 in the negative regulation of p53 by Mdm2. *EMBO J.* **18**, 1805–1814.

Weber, J.D., Kuo, M.-L., Bothner, B., *et al.* (2000) Cooperative signals Governing ARF-Mdm2 interaction and nucleolar localization of the complex. *Mol. Cell. Biol.* **20**, 2517–2528.

Weber, J.D., Taylor, L.J., Roussel, M.F., Sherr, C.J. & Bar-Sagi, D. (1999) Nucleolar Arf sequesters Mdm2 and activates p53. *Nature Cell Biol.* **1**, 20–26.

Wu, X., Henri Bayle, J., Olson, D. & Levine, A.J. (1993) The p53-mdm-2 autoregulatory feedback loop. *Genes Dev.* **7**, 1126–1132.

Wymann, M.P., Bulgarelli-Leva, G., Zvelebil, M.J., *et al.* (1996) Wortmannin inactivates phophinositide 3-kinase by covalent modification of Lys-802, a residue involved in the phosphate transfer reaction. *Mol. Cell. Biol.* **16**, 1722–1733.

Yih, L.-H. & Lee, T.-C. (2000) Arsenite induces p53 accumulation through an ATM-dependent pathway in human fibroblasts. *Cancer Res.* **60**, 6346–6352.

Zauberman, A., Lupo, A. & Oren, M. (1995) Identification of p53 target genes through immune selection of genomic DNA: the cyclin G gene contains two distinct p53 binding sites. *Oncogene* **10**, 2361–2366.

Zhang, Y., Xiong, Y. & Yarbrough, W.G. (1998) ARF promotes MDM2 degradation and stabilizes p53: ARF-INK4a locus deletion impairs both the Rb and p53 tumor suppression pathways. *Cell* **92**, 725–734.

Received: 7 May 2002
Accepted: 22 May 2002

DNA RESEARCH 9, 209–215 (2002)

Abundant Poly(A)-Bearing RNAs That Lack Open Reading Frames in *Schizosaccharomyces pombe*

Takanori WATANABE, Kazuyuki MIYASHITA, Takamune T. SAITO, Kentaro NABESHIMA, and Hiroshi NOJIMA*

Department of Molecular Genetics, Research Institute for Microbial Diseases, Osaka University, 3-1 Yamadaoka, Suita City, Osaka 565-0871, Japan

(Received 18 October 2002; revised 25 November 2002)

Abstract

We report here that 6.9% (68/987) of randomly selected cDNA clones from an *S. pombe* cDNA library lack apparently long open reading frames which we denote *prl*. One of them, *prl1*, was examined further because multiple bands were observed when it was used as a probe in northern blot analysis. These multiple bands appear to be derived from overlapping transcripts from both DNA strands, including non-coding RNAs and antisense RNAs in addition to mRNA. Such mechanisms may increase the transcriptional variation in *S. pombe* cells.

Key words: non-coding RNA; anti-sense RNA; overlapping transcripts; multiplex transcription; *S. pombe*

Eukaryotic genomes adopt the following strategies to increase the variation of transcripts; overlapping transcription derived from both strands,[1,2] overlapping reading frame in one strand,[3] transcripts derived from an intron of another transcript,[4] alternative splicing, *trans*-splicing[5–8] and translational frame shifting.[9] The production of non-coding/antisense RNAs that do not code for proteins also increases the transcriptional repertoire. Non-coding RNAs have been found in many organisms and are known to play critical roles in many biological phenomena.[10–12] In humans and *Drosophila*, non-coding RNAs are important in the regulation of dosage compensation in X chromosome.[13,14] In mice, H19 RNA expressed maternally are essential, acting negatively for growth, whereas Igf2 expressed paternally acts positively for growth.[15]

In *S. pombe*, binding of meiRNA to Mei2 protein is required for progression in meiosis I, which promotes translocation of Mei2 protein from the cytoplasm to the nucleus.[16,17] The coding region of *spo6*$^+$ is transcribed bi-directionally,[18] and three kinds of transcript of the complementary strand of *rec7*$^+$ have been detected.[19] The complete genome sequence of *S. pombe*[20] revealed 4824 annotated protein-coding genes, the smallest among eukaryotes examined to date, amounting to only 85% of the number found in the budding yeast *S. cerevisiae*. The following possibilities were considered to explain this finding: 1) there are fewer duplicated genes (361) than that in *S. cerevisiae* (716), and 2) the distance between the protein-coding regions is generally longer than that in *S. cerevisiae*, and this may contribute to the complex regulation of gene expression.

Previously, we isolated 31 kinds of meiosis-specific transcripts named *meu* in *S. pombe* by a cDNA subtraction method.[21] Unexpectedly, 5 out of the 31 *meu* transcripts were estimated to be non-coding/antisense RNAs. Since this finding seems important, we searched for more examples of such non-coding/antisense RNAs in *S. pombe*. Here, we report isolation of cDNA for 68 non-coding/antisense RNAs as well as an example of multiply overlapping transcripts in *S. pombe*.

Of the 987 different cDNA clones, we randomly selected and sequenced cells that are either in mitotic growth phase or in meiosis from a cDNA library prepared using mRNA transcribed in *S. pombe* (see legend for Fig. 1). We found 68 unique clones lacking significant open reading frames (ORFs) that appear to generate non-coding or antisense RNAs species. We denoted these clones *prl* (*poly(A)-bearing RNA without long open reading frames*). Here, "long" means 100 or more amino acids except for *prl25*, which is an antisense RNA of SPBC29A10. Figure 1 demonstrates the locations in the *S. pombe* genome from which these *prl* clones are derived as well as the direction of their transcription (Table 1). The potential CDSs (protein-coding sequence) around these *prl* transcripts as determined by the

Communicated by Hideo Shinagawa

* To whom correspondence should be addressed. Tel. +81-6-6875-3980, Fax. +81-6-6875-5192, E-mail: hnojima@biken.osaka-u.ac.jp

† The sequences reported here have been deposited in the DDBJ database under accession numbers AB084813 to AB084880.

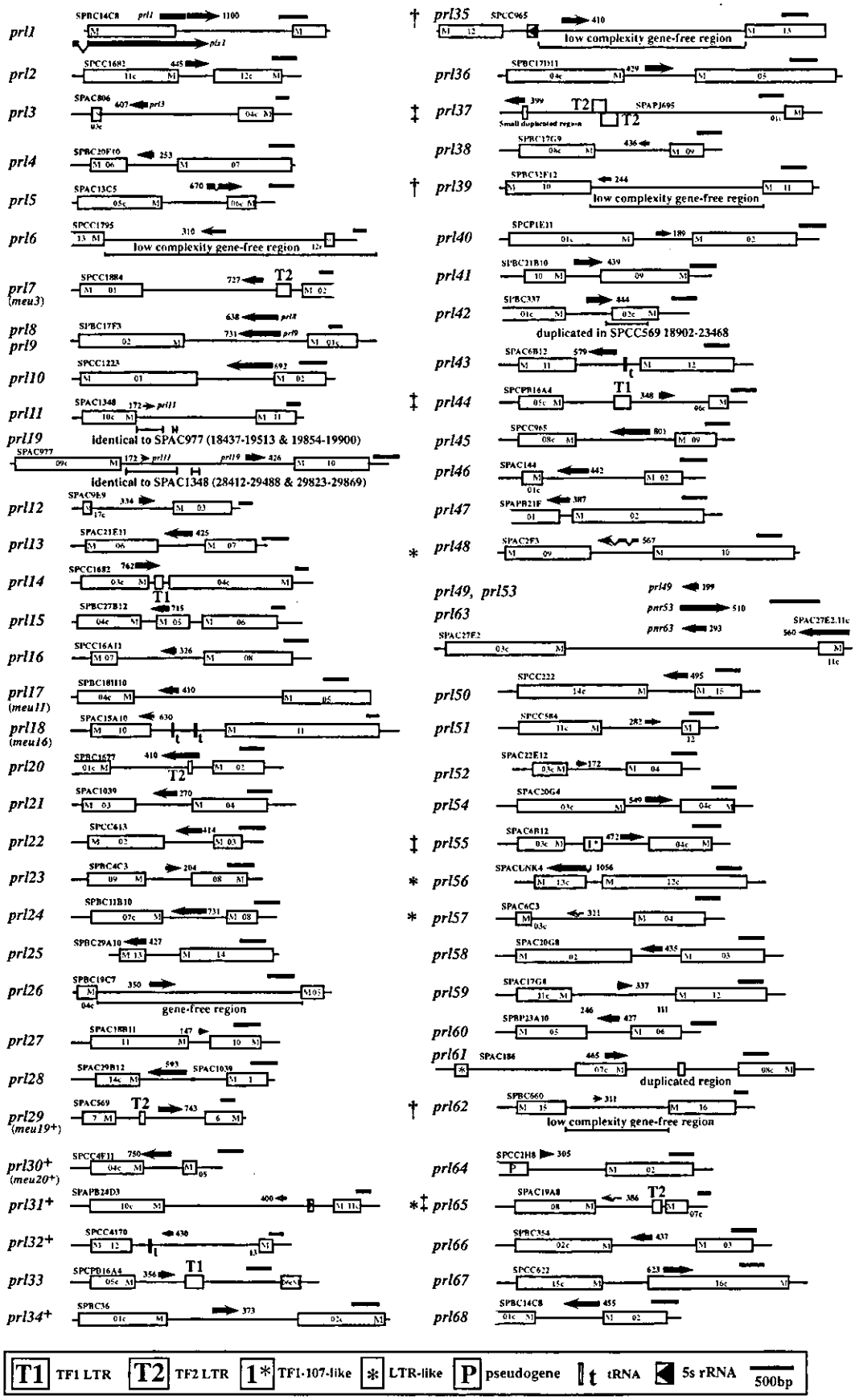
prl1
prl2
prl3
prl4
* prl5
† prl6
low complexity gene-free region
‡ prl7 (meu3)
T2
prl8
prl9
prl10
prl11
prl19
identical to SPAC977 (18437-19513 & 19854-19900)
identical to SPAC1348 (28412-29488 & 29823-29869)
prl12
prl13
‡ prl14
T1
prl15
prl16
prl17 (meu11)
prl18 (meu16)
‡ prl20
T2
prl21
prl22
prl23
prl24
prl25
† prl26
gene-free region
prl27
prl28
‡ prl29 (meu19+)
T2
prl30+ (meu20+)
prl31+
prl32+
‡ prl33
T1
prl34+
† prl35
low complexity gene-free region
prl36
‡ prl37
T2
T2
prl38
† prl39
low complexity gene-free region
prl40
prl41
prl42
duplicated in SPCC569 18902-23468
prl43
‡ prl44
T1
prl45
prl46
prl47
* prl48
prl49, prl53
prl63
prl50
prl51
prl52
prl54
‡ prl55
* prl56
* prl57
prl58
prl59
prl60
prl61
duplicated region
† prl62
low complexity gene-free region
prl64
*‡ prl65
T2
prl66
prl67
prl68
T1 TF1 LTR
T2 TF2 LTR
1* TF1-107-like
* LTR-like
P pseudogene
t tRNA
5s rRNA
500bp

DNA sequence database of *S. pombe* (The Sanger Centre, UK) are shown by boxes with the initiation methionine sites indicated (M) (Fig. 1). We noticed that the Sanger Centre database also contains 43 non-coding RNA species that are annotated as 'mRNA-like miscellaneous RNA' based on comparison of the genomic database with the cDNA clone database. We denoted these species as *prl* here for convenience.

Curiously, several of the *prl*s (*prl5*, *prl48*, *prl56*, *prl57*, and *prl65*) have introns. The maximum ORFs of these *prl*s would code for small proteins that are 29, 85, 70, 25, and 18 amino acids long, respectively. These sequences could actually be translated into these small proteins since the putative peptide from *prl48* has weak similarity to the 49C12.12p protein of *Caenorhabditis elegans*. However, as it is known that the U6 snRNA gene of *S. pombe* also has an intron,[22] these *prl*s could also be such intron-charged non-coding RNA genes.

Using Zuker's computer program with the parameters in the algorithm presented in Jaeger et al.,[23] we found that all of the 68 *prl* transcripts form stable hairpin structures (data not shown), suggesting the idea that the gene products are stable RNA molecules. It is noteworthy that about 20% (14 of the 68 clones) of the *prl* transcripts are derived from gene-free regions of the *S. pombe* genome or near the repetitive sequence, long terminal repeat (LTR). They are indicated in Fig. 1 by daggers (†) and double daggers (‡), respectively. The *prl11* sequence is found in both SPAC1348 and SPAC977, and this is probably a case of transcriptional duplication as is the case of *meu3*$^+$ (*prl7*) and *meu19*$^+$ (*prl29*).[21]

We chose *prl1* for further analysis because multiple bands were observed when it was used as a probe in northern blot analysis for *S. pombe* RNA. We dissected the genomic DNA fragment around the *prl1* region with appropriate restriction enzymes to generate the DNA fragments denoted a–i (Fig. 2A). Northern blot analysis using these fragments as probes showed that the probes detected two or more bands with distinct sizes and various patterns for appearance and disappearance in mitotic or meiotic cells (Fig. 2B). The longest transcript, which is 5.8 kb, appears to contain two ORFs (Plx1 and Pac2). The downstream ORF coincides with Pac2 that controls the onset of sexual development.[24] Thus, the 5.8-kb transcript may be a bicistronic mRNA. Transcripts of smaller sizes (less than 0.8 kb) are expected to harbor no apparent ORFs longer than 30 amino acids. Genomic Southern blot analysis using the DNA fragments from this region as probes reveals that the probes all recognize a single band. Thus, it is not likely that the multiple bands in the northern blots arise from cross-reaction with transcripts from other genomic regions (Fig. 2C).

To accurately identify the size of these transcripts and the direction they are transcribed, we screened the cDNA library[21] (see legend for Fig. 1) by colony hybridization and isolated five different cDNA clones that may correspond to each transcript (Table 2). These cDNA clones are called *plx1* to *plx5* after *multiplex transcripts* (Fig. 2A). The *plx1* transcript encodes a protein (Plx1) that is homologous to the Myb-like transcriptional factor. A cDNA clone for *prl1* is not the partial cDNA clone of *plx1* because the band at 1.1 kb by northern blot (Fig. 2B) for *prl1* is detected only when probe e or f is used. It is also unlikely that the 1.1-kb transcript is a breakdown product because the time course of transcription is distinct from that of *plx1* transcript (2.6 kb) which is meiosis specific (Fig. 2B-b, c, and d). *plx2* is a small transcript with its end in the intron of *plx1*. It remains to be examined whether *plx2* is the breakdown product derived from the mRNA precursor of *plx1*. We failed to obtain the cDNA for the longest sense transcript (*plx6*) that corresponds to the band at 5.8 kb (Fig. 2B-c–h).

It is notable that *plx3*, *plx4*, and *plx5* cDNA clones are derived from the antisense RNAs of *plx1*. Namely, *plx3*, *plx4*, and *plx5* transcripts cannot be the breakdown products of *plx1*. The facts that northern blot confirms that these cDNAs are transcribed (Fig. 2B-c, d, and e) and that each cDNA clone has a poly(A) tail about 30 nucleotides downstream of the putative poly(A) signal (AAUAAN) indicate that these cDNAs are not the artifacts generated during the cDNA preparation.[21] We also detected similar kinds of antisense RNAs in the *rec7*$^+$ gene region, previously.[19] It remains to be examined whether these antisense transcripts are functional gene products or merely the junk mRNA-like transcripts.

The upstream region of *plx1* contains a TR-box sequence that is also contained in the target sequence of Ste11,[25] a transcriptional factor that regulates the entry of the cells into meiosis. As shown in Fig. 2B, the expression profiles of each transcript in northern blot differ. Expression of the 5.8-kb (*plx6*) and 2.6-kb (*plx1*) bands appear 4 h after nitrogen starvation in a meiosis-specific manner. Their levels peak at 6 h and then decrease. In contrast, *prl1* (1.1 kb), *plx3* (0.8 kb), *plx4* (0.4 kb),

Figure 1. The locations and the directions of the *prl* transcripts in the *S. pombe* genome. The sharp end of each horizontal arrow denotes the location of the poly(A) tail for each *prl* transcript. The numbers beside the arrows are the estimated sizes of the isolated cDNA inserts (nucleotides). Each bar indicates 500 base pairs. The T1, T2, 1$^{\text{asterisk}}$, asterisk, P and filled triangle in the box indicated TF1-LTR (LTR retrotransposon of the Tf1/sushi group), TF2-LTR (LTR retrotransposon of the Tf2 group), TF1-107-like LTR, LTR-like, pseudogene and 5s rRNA, respectively. The filled rectangle near the t indicates tRNA. Asterisks, daggers and double daggers signify the *prl*s that harbor introns, that locate in the gene-free region and that situate near the LTR of the *S. pombe* genome, respectively. To make *S. pombe* cDNA libraries that are derived from mRNA transcribed in both mitotic and meiotic cells, CD16-1 (*h*$^+$/*h*$^-$ *ade6M-210/ade6-M216 cyh1/++/lys5-391*) cells were directed to meiosis by nitrogen starvation and collected at one hour intervals (1, 2, 3, 4, 5, 6 hrs).[21] Note that not all cells proceed to meiosis under this condition, and a part of the cell population remains at the mitotic phase. Using poly(A) plus RNA purified from these cells, the cDNA library was constructed by a linker-primer method with the pAP3neo vector, as described previously.[30]

Table 1. Characterization of *prl* genes.

Name	Cosmid number	Genomic sequence	Class	Amino acids	Base	Inter CDS	Accession #
prl01	SPAC31G5.10/11	14046(14518)→15146	Non-coding	48	1100	2371	AB084813
prl02	SPCC1682.11c/12c	24926→25370	Non-coding	51	445	699	AB084814
prl03	SPAC806.03c/04c	7406→6800	Non-coding	72	607	5410	AB084815
prl04	SPBC20F10.06/07	12596→12344	Non-coding	43	253	1021	AB084816
prl05	SPAC13C5.06c A/S	9962→10125, 10196→10701	Antisense	29	668	1320*	AB084817
prl06	SPCC1795.13/12C	5143→4834	Non-coding	36	310	8851†	AB084818
prl07/meu3	SPCC1884.01/02	9595→8852	Non-coding	36	727	5065‡	AB084819
prl08	SPBC17F3.02/01c	5638→5000	Non-coding	45	638	2486	AB084820
prl09	SPBC17F3.02/01c	5742→5012	Non-coding	45	731	2486	AB084821
prl10	SPCC1223.01/02	5037→4346	Non-coding	49	692	1570	AB084822
prl11	SPAC1348.10c/11, SPAC977.09c/10	28624→28796	Non-coding	23	172	4858	AB084823
prl12	SPAC9E9.17c/03	4375→4708	Non-coding	10	334	2941	AB084824
prl13	SPAC21E11.06/07	9944→9520	Non-coding	15	425	961	AB084825
prl14	SPAC1486.03c/04c	7001→7762	Antisense	69	762	961‡	AB084826
prl15	SPBC27B12.05 A/S	7546→6832	Antisense	22	715	611	AB084827
prl16	SPCC16A11.07/08	15361→15045	Non-coding	30	326	1731	AB084828
prl17/meu11	SPBC18H10.04c/05	10576→10163	Non-coding	38	410	3116	AB084829
prl18/meu16	SPAC15A10.10 A/S	23807→23178	Antisense	14	630	2957/827	AB084830
prl19	SPAC977 09c/10	21395→21820	Non-coding	34	426	3956	AB084831
prl20	SPBC1677.01c/02	2394→1942	Non-coding	38	410	2030‡	AB084832
prl21	SPAC1039.03/04	10523→10254	Non-coding	3	270	1146	AB084833
prl22	SPCC613.02/03	5296→4883	Non-coding	23	414	1009	AB084834
prl23	SPBC4C3.09/08	5926→6129	Non-coding	14	204	928	AB084835
prl24	SPBC11B10.07c/08	12246→11516	Non-coding	99	731	1309	AB084836
prl25	SPBC29A10.13 A/S	34312→34738	Antisense	102	427	709	AB084837
prl26	SPBC19C7.04c/05	14485→14834	Non-coding	19+19	350	4122†	AB084838
prl27	SPAC18B11.11/10	4985→5131	Non-coding	17	147	841	AB084839
prl28	SPAC29B12.14c/SPAC1039.01	36000→35407	Non-coding	19	593	3756	AB084840
prl29/meu19	SPCC569.07/06	6657→7399	Non-coding	36	743	3602‡	AB084841
prl30/meu20	SPCC4F11.04c/-	8882→8278	Non-coding	36	750	1305	AB084842
prl31	SPAPB24D3.10c/11c	26459→26060	Non-coding	49	400	6822/5801	AB084843
prl32	SPCC417.12/13	34568→34139	Non-coding	43	430	5159/4489	AB084844
prl33	SPCPB16A4.05c/06c	11431→11786	Non-coding	6	356	2887‡	AB084845
prl34	SPBC36.01c/2c	4806→5178	Non-coding	15	373	2647	AB084846
prl35	SPCC965.12/13	31707→32116	Non-coding	58	410	4937/4160†	AB084847
prl36	SPBC17D11.04c/5	9240→9668	Non-coding	9	429	1457	AB084848
prl37	SPAPJ695.-/01c	1905→1507	Non-coding	21	399	8639‡	AB084849
prl38	SPBC17G9.08c/09	20116→19682	Non-coding	64	436	3035	AB084850
prl39	SPBC32F12.10/11	19419→19176	Non-coding	50	242	3455†	AB084851
prl40	SPCP1E11.01c/02	4408→4598	Non-coding	19	189	1200	AB084852
prl41	SPBC21B10.10/09	17800→18238	Non-coding	12+12	439	708	AB084853
prl42	SPBC337.01c/02	1662→2109	Non-coding	28	444	918	AB084854
prl43	SPAC6B12.11/12	26150→25569	Non-coding	66	579	1284/940	AB084855
prl44	SPCPB16A4.05c/06c	12868→13215	Non-coding	37	348	2887‡	AB084856
prl45	SPCC965.08/09	21539→20737	Non-coding	24	801	2005	AB084857
prl46	SPAC144.01c/02	1527→1086	Non-coding	18	442	2030	AB084858
prl47	SPAPB21F2.01A/S	1483→1098	Antisense	40	387	480	AB084859
prl48	SPAC2F3.09/10	20491→20360, 20258→20089, 19949→19713	Non-coding	85	552	1254*	AB084860
prl49	SPAC27E2.03c/11c	7812→7614	Non-coding	33	199	2544	AB084861
prl50	SPACC222.14c/15	34830→34337	Non-coding	19	495	975	AB084862
prl51	SPCC584.11c/12	14047→14328	Non-coding	18	282	1598	AB084863
prl52	SPAC22E12.03C/04	3719→3890	Non-coding	46	172	1183	AB084864
prl53	SPAC27E2.03C/11c	7602→8111	Non-coding	21	510	2544	AB084865
prl54	SPAC20G4.02C/03C	8631→9179	Non-coding	64	549	1117	AB084866
prl55	SPAC6B12.03c/04c	9463→9934	Non-coding	73	472	1644‡	AB084867
prl56	SPACUNK4.13c A/S	15893→15892, 15804→14771	Antisense	70	1055	317*	AB084868
prl57	SPAC6C3.03c/04	8572→8493, 8441→8201	Non-coding	25	321	2040*	AB084869
prl58	SPAC20G8.02/03	4265→3819	Non-coding	30	435	989	AB084870
prl59	SPAC17G8.11c/12	18820→19156	Non-coding	27	337	2054	AB084871
prl60	SPBP23A10.05/06	8007→7581	Non-coding	36	427	868	AB084872
prl61	SPAC186.07c A/S	21421→21885	Antisense	38	465	2270	AB084873
prl62	SPBC660.15/16	35312→35700	Non-coding	30	311	4128†	AB084874
prl63	SPAC27E2.03C/11c	7853→7614	Non-coding	33	239	2544	AB084875
prl64	SPCC2H8.psudo/02	499→791	Non-coding	6+6	293	1520	AB084876
prl65	SPAC19A8.08/07c	16608→16572, 16460→16110	Non-coding	18	388	2773*‡	AB084877
prl66	SPBC354.02c/03	3008→3444	Non-coding	48	437	1703	AB084878
prl67	SPCC622.16c A/S	30852→31474	Antisense	39	623	919	AB084879
prl68	SPBC14C8.01c/02	1735→1281	Non-coding	33	455	1332	AB084880

Inter CDS (protein coding sequence) signifies the length between the CDS that are registered in the database of Sanger Center.

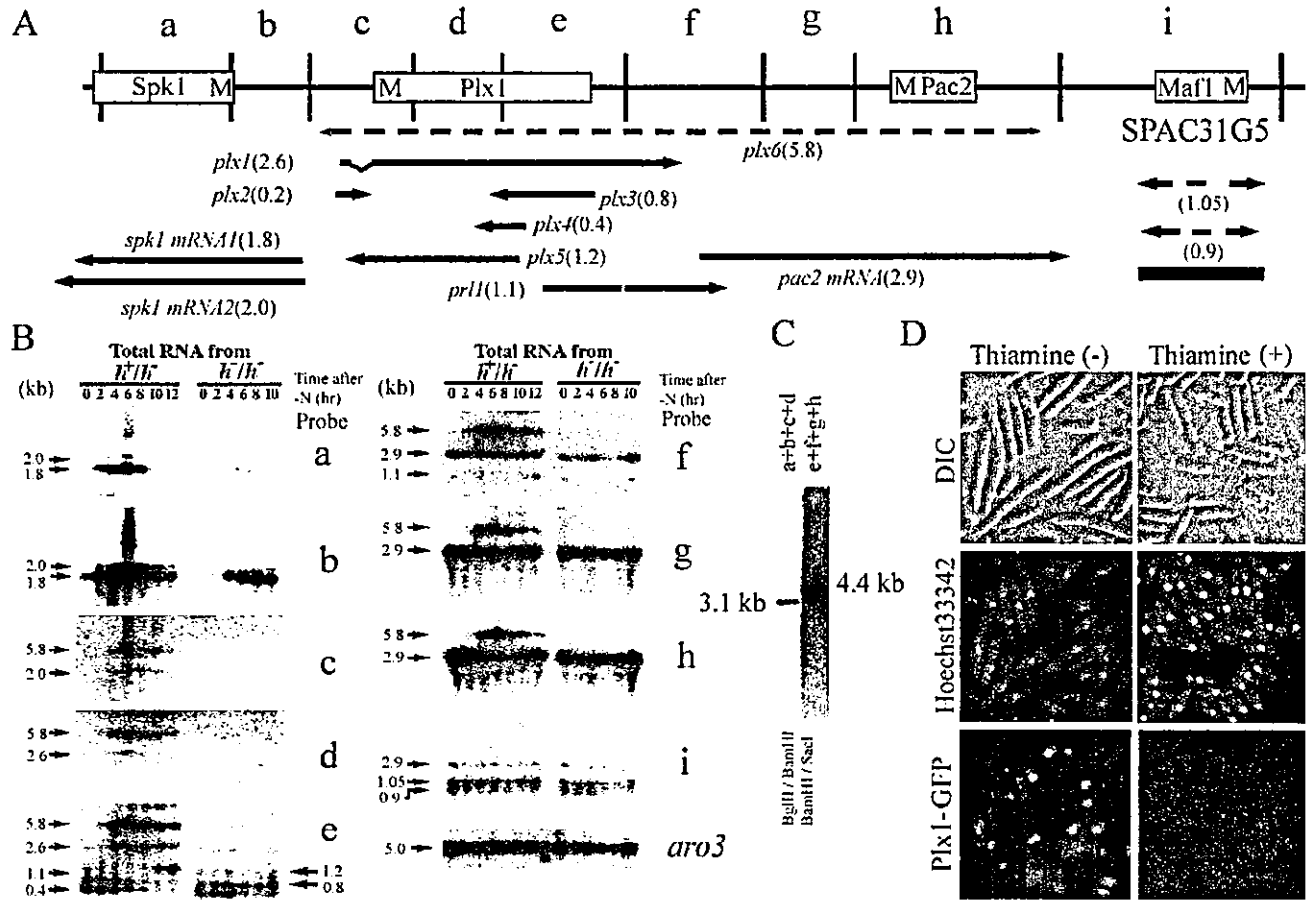

Figure 2. Isolation and characterization of multiplex RNA species in the genome of *S. pombe*. (A) A schematic presentation of the regions around the genomic fragment of the *plx1*$^+$ gene that transcribes *plx1* mRNA and encodes Plx1 protein, showing its multiplex transcription. The locations and directions of the isolated cDNA inserts are indicated by thick horizontal arrows. Boxes represent potential CDSs as assessed in the database (The Sanger Centre, UK). The initiation methionine site (M) in these CDSs is indicated. The bar indicates 1000 base pairs. Accession numbers for the *plxes* are registered as AB084881–AB084888 (See also Table 2). (B) Northern blot analyses using the DNA fragment around the *prl1* transcript. [α-^{32}P]dCTP probes were used as described before.[21] The locations of the nine different DNA fragments (a–i) used as probes are shown above. Thick horizontal arrows denote the orientation and size of the cDNA clones. The amount of loaded RNA was monitored by using the ^{32}P-labeled *aro3*$^+$ gene probe. (C) Southern blot analysis of whole genomic *S. pombe* DNA digested with relevant restriction enzymes. The probes consisted of two pools of probes (a + b + c + d and e + f + g + h). (D) Microscopic views of the enlarged cells generated by ectopically expressing *plx1* cDNA fused with *gfp* gene in mitotic cells. Shown are DIC (differential interference contrast) and fluorescence photographs of Hoechst33342-stained cells or *plx1*$^+$-*gfp*-bearing cells. Fluorescence from GFP-Plx1 fusion protein was observed predominantly in the nucleus only when the *nmt* promotor was induced by depletion of thiamine. The profiles of meiotic progression after nitrogen starvation using CD16-1 and CD16-5 (*h*$^-$/*h*$^-$ *ade6-M210/ade6-M216 cyh1/++/lys5-391*) strains were reported previously.[21]

and *plx5* (1.2 kb) are expressed not only during meiosis but also at 0 h when cells are in the mitotic phase. Thus, these latter transcripts are not specifically produced during meiosis alone.

It is interesting to note that, in the heterozygous strain CD16-1 that enters meiosis, the expression level of the antisense RNA species (*plx3* and *plx4*) decreases as the amount of the sense transcript (*plx1*) increases. However, the levels of *plx3* and *plx4* transcripts do not change in the homozygous strain CD16-5 that does not enter meiosis after nitrogen starvation. This suggests that the Plx1 protein may be harmful for mitotic cell growth. To test this possibility, we examined mitotic cells carrying *plx1* cDNA fused with green fluorescent protein (gfp) gene whose expression is driven by the *nmt* promoter. After 22 h of thiamine depletion to induce the activity of the *nmt* promoter, enlarged cells were observed under a microscope (Fig. 2D). This suggests that the expression of *plx1* mRNA in mitosis may indeed be harmful to the cell.

In the vicinity of *plx1*, other genes such as *spk1*$^+$ (SPAC5G10.9c), *pac2*$^+$ (SPAC5G10.11) and *maf1*$^+$ (SPAC5G10.12c) also display two, two and three bands in northern blots (Fig. 2B, probe a, h, and i), respectively. We have isolated two kinds of cDNA clones that are derived from the region of the Spk1 protein-coding

Table 2. List of transcripts in the vicinity of *prl1*$^+$ genes.

Name	class	site (SPAC31G5)	TR-box	TATA-box	polyA additional signal	b.p.	A. N.
prl1 *	non-coding	14518-15146		13992TATAAT/14131TATAAT	15122AATAAt	629	AB084813
plx1+	mRNA	11986-12034 12269-14773	11927TTCTTTGTTT	11777 TATAAc	14748AATAAA	2554	AB084881
plx2 *	non-coding	11991-12160		11777 TATAAc	12132AATAAt	170	AB084882
plx3 *	antisense	13988-13206		14257TATAAa	13222AATAAc/13229AATAAt	783	AB084883
plx4 *	antisense	13485-13064		14257TATAAa	13085AATAAg	422	AB084884
plx5 *	antisense	13333-12055		14257TATAAa/15007TATAtt	12119AATtAA	1279	AB084885
spk1+	mRNA1	11715-9893		11780TATAAa	9919AATAAA	1823	AB084886
spk1+	mRNA2	11723-9776		11780TATAAa	9799AATgAA	1948	AB084887
pac2+	mRNA	14854-17761		14623gATAAT	17727AATAcA	2908	AB084888

region and that have different poly(A) sites. The variation in the size of the 3′ UTR may also be caused by post-transcriptional regulation.[26] Furthermore, we found that *prl49*, *prl53*, and *prl63* are derived from the same genomic region in SPAC27E2 (Fig. 1). Northern blots using this region as a probe also showed three bands that are not meiosis-specific (data not shown), representing another case of multiplex transcription.

Whole genome DNA sequencing of *S. pombe* revealed that the spaces between protein coding genes are longer than that of *S. cerevisiae*. About ten gene-free regions per chromosome are found, which are usually flanked by tandemly oriented genes. It has been pointed out that one of them corresponds to a prominent meiotic DNA break site or cluster of such sites.[20] The average length of the spaces between the genes (including ORFs, tRNA, or rRNA) where *prl* transcripts (*prl1–prl68*) are detected is 2483 bp. This value is larger than that of the average length of the spaces between the genes in the whole genome (about 900 bp for *S. pombe* and 800 bp for *S. cerevisiae*). The result indicates that *prl* transcripts are preferentially situated in longer inter-CDS regions to increase the variation of gene expression in *S. pombe*.

It should be borne in mind, of course, that such poly(A)-bearing RNAs without long ORFs may encode small peptides because the smallest protein-coding gene so far identified encodes an amino acid only 7 peptides long.[27] The annotated *S. pombe* genes includes the 147 genes that are confirmed or predicted to encode proteins of 25–99 amino acids, and the 116 genes that are treated as low coding potential because the gene products are too small to display any significant homology. Notably, our *prl* transcripts are not included in any of these categories.

Considering that we identified *prl* transcripts by cDNA clonings and they represent only a part of such clones in the cDNA library, it is evident that a large number of such non-coding poly(A)-bearing RNAs are transcribed in *S. pombe* cells and the corresponding cDNA clones remain to be discovered. Since we have isolated 68 kinds of *prl* transcripts from 987 randomly selected cDNA clones in the library (6.9%), we surmise that nearly 300 *prl* transcripts remain undiscovered. It should be pointed out that functional analysis of such non-coding RNAs has escaped classical genetics analysis so far, because genes without protein-coding regions tended to be ignored. In *S. pombe*, meiRNA is an exceptional case, which is shown to be essential for commitment of meiosis.[16] We therefore anticipate that many non-coding RNAs will be rediscovered among the ignored functional genes.

Considering that positional cloning in human genetics has identified non-coding RNA species as the cause of cartilage-hair hypoplasia[28] and autosomal-dominant congenital dyskeratosis,[29] it is probable that *prl* transcripts play a variety of roles in many aspects of cellular function. DNA chip array analysis targeting the *prl* transcripts would be helpful to analyze their functions, thus complementing the functional genomic analysis of *S. pombe*.

Acknowledgements: We thank Profs. C. Shimoda, M. Yamamoto, M. Yanagida, and Dr. Y. Watanabe for the *S. pombe* strains and plasmids, and Dr. Valerie Wood for the gift of cosmid clones. This work was supported by Grant-in-Aid for Scientific Research on Priority Areas (C) "Genome Biology" from the Ministry of Education, Culture, Sports, Science and Technology of Japan to HN. TW is a Research Fellow of the Japan Society for the promotion of Science.

References

1. Adelman, J. P., Bond, C. T., Douglass, J., and Herbert, E. 1987, Two mammalian genes transcribed from opposite strands of the same DNA locus, *Science*, **235**, 1514–1517.
2. Williams, T. and Fried, M. 1986, A mouse locus at which transcription from both DNA strands produces mRNAs complementary at their 3′ ends, *Nature*, **322**, 275–279.
3. Kozak, M. 2001, Extensively overlapping reading frames in a second mammalian gene, *EMBO Rep.*, **2**, 768–769.
4. Henikoff, S., Keene, M. A., Fechtel, K., and Fristrom, J. W. 1986, Gene within a gene: nested *Drosophila* genes encode unrelated proteins on opposite DNA strands, *Cell*, **44**, 33–42.
5. Casci, T. 2001, RNA splicing. Chance findings, *Nat. Rev. Genet.*, **2**, 162.
6. Labrador, M., Mongelard, F., Plata-Rengifo, P., Baxter, E. M., Corces, V. G., and Gerasimova, T. I. 2001, Protein encoding by both strands, *Nature*, **409**, 1000.
7. Nilsen, T. W. 2001, Evolutionary origin of SL-addition *trans*-splicing: still an enigma, *Trends Genet.*, **17**, 678–

680.
8. Mongelard, F., Labrador, M., Baxter, E. M., Gerasimova, T. I., and Corces, V. G. 2002, Trans-splicing as a novel mechanism to explain interallelic complementation in *Drosophila*, *Genetics*, **160**, 1481–1487.
9. Matsufuji, S., Matsufuji, T., Miyazaki, Y. et al. 1995, Autoregulatory frameshifting in decoding mammalian ornithine decarboxylase antizyme, *Cell*, **80**, 51–60.
10. Eddy, S. R. 2001, Non-coding RNA genes and the modern RNA world, *Nat. Rev. Genet.*, **12**, 919–929.
11. Mattick, J. S. 2001, Non-coding RNAs: the architects of eukaryotic complexity, *EMBO Rep.*, **11**, 986–991.
12. Moss, E. G. 2000, Non-coding RNA's: lightning strikes twice, *Curr. Biol.*, **10**, 436–439.
13. Brown, C. J., Ballabio, A., Rupert, J. L. et al. 1991, A gene from the region of the human X inactivation centre is expressed exclusively from the inactive X chromosome, *Nature*, **349**, 38–44.
14. Franke, A. and Baker, B. S. 1999, The rox1 and rox2 RNAs are essential components of the compensasome, which mediates dosage compensation in *Drosophila*, *Mol. Cell*, **4**, 117–122.
15. Wolffe, A. P. 2000, Transcriptional control: imprinting insulation, *Curr. Biol.*, **10**, 463–465.
16. Watanabe, Y. and Yamamoto, M. 1994, *S. pombe mei2*$^+$ encodes an RNA-binding protein essential for premeiotic DNA synthesis and meiosis I, which cooperates with a novel RNA species meiRNA, *Cell*, **78**, 487–498.
17. Yamashita, A., Watanabe, Y., Nukina, N., and Yamamoto, M. 1998, RNA-assisted nuclear transport of the meiotic regulator Mei2p in fission yeast, *Cell*, **95**, 115–123.
18. Nakamura, T., Kishida, M., and Shimoda, C. 2000, The *Schizosaccharomyces pombe spo6*$^+$ gene encoding a nuclear protein with sequence similarity to budding yeast Dbf4 is required for meiotic second division and sporulation, *Genes Cells*, **6**, 463–479.
19. Molnar, M., Parisi, S., Kakihara, Y. et al. 2001, Characterization of REC7, an early meiotic recombination gene in *Schizosaccharomyces pombe*, *Genetics*, **157**, 519–532.
20. Wood, V., Gwilliam, R., Rajandream, M. A. et al. 2002, The genome sequence of *Schizosaccharomyces pombe*, *Nature*, **415**, 871–880.
21. Watanabe, T., Miyashita, K., Saito, T. T. et al. 2001, Comprehensive isolation of meiosis-specific genes identifies novel proteins and unusual non-coding transcripts in *Schizosaccharomyces pombe*, *Nucleic Acids Res.*, **29**, 2327–2337.
22. Tani, T. and Ohshima, Y. 1989, The gene for the U6 small nuclear RNA in fission yeast has an intron, *Nature*, **337**, 87–90.
23. Jaeger, J. A., Turner, D. H., and Zuker, M. 1989, Improved predictions of secondary structures for RNA, *Proc. Natl. Acad. Sci. U.S.A.*, **86**, 7706–7710.
24. Kunitomo, H., Sugimoto, A., Wilkinson, C. R., and Yamamoto, M. 1995, *Schizosaccharomyces pombe pac2*$^+$ controls the onset of sexual development via a pathway independent of the cAMP cascade, *Curr. Genet.*, **28**, 32–38.
25. Sugimoto, A., Iino, Y., Maeda, T., Watanabe, Y., and Yamamoto, M. 1991, *Schizosaccharomyces pombe ste11*$^+$ encodes a transcription factor with an HMG motif that is a critical regulator of sexual development, *Genes Dev.*, **11**, 1990–1999.
26. Edwalds-Gilbert, G., Veraldi, K. L., and Milcarek, C. 1997, Alternative poly(A) site selection in complex transcription units: means to an end?, *Nucleic Acids Res.*, **25**, 2547–2561.
27. Gonzalez-Pastor, J. E., San Millan, J. L., and Moreno, F. 1994, The smallest known gene, *Nature*, **369**, 281.
28. Ridanpaa, M., van Eenennaam, H., Pelin, K. et al. 2001, Mutations in the RNA component of Rnase MRP cause a pleiotropic human disease, cartilage-hair hypoplasia, *Cell*, **104**, 195–203.
29. Vulliamy, T., Marrone, A., Goldman, F. et al. 2001, The RNA component of telomerase is mutated in autosomal dominant dyskeratosis congenital, *Nature*, **413**, 432–435.
30. Kobori, M., Ikeda, Y., Nara, H. et al. 1998, Large scale isolation of osteoclast-specific genes by an improved method involving the preparation of a subtracted cDNA library, *Genes Cells*, **3**, 459–475.

ELSEVIER

International Immunopharmacology 2 (2002) 631–640

International Immunopharmacology

www.elsevier.com/locate/intimp

Regulation of human B cell function by sulfasalazine and its metabolites

Shunsei Hirohata*, Nobuharu Ohshima, Tamiko Yanagida, Kaori Aramaki

Department of Internal Medicine, Teikyo University School of Medicine, 2-11-1 Kaga, Itabashi-ku, Tokyo 173-8605, Japan

Received 27 August 2001; accepted 6 November 2001

Abstract

Although sulfasalazine is a well-known disease-modifying antirheumatic drug (DMARD), the mechanisms of its action remain unclear. Indeed, it remains uncertain whether sulfasalazine itself or one of its metabolites is responsible for the antirheumatic effects of sulfasalazine. Since one of the characteristic features of rheumatoid arthritis (RA) is chronic stimulation of B cells, we compared the effects of sulfasalazine and its metabolites on the in vitro function of human B cells. Ig production was induced from highly purified B cells from healthy donors by stimulation with *Staphylococcus aureus* Cowan I (SA) plus IL-2. Sulfasalazine suppressed the production of IgM and IgG at its pharmacologically attainable concentrations (1–10 μg/ml). Of the metabolites of sulfasalazine, sulfapyridine (SP) and 5-aminosalicylic acid (5-ASA), but not 4-acethyl SP, also significantly suppressed the production of IgM and IgG at their pharmacologically relevant concentrations. By contrast, any of sulfasalazine, SP, 5-ASA and 4-acethyl SP did not suppress the IFN-γ production of immobilized anti-CD3 stimulated CD4+ T cells. These results indicate that sulfasalazine and its metabolites preferentially suppress the function of B cells, but not that of T cells, at their pharmacologically attainable concentrations. The data therefore suggest that not only sulfasalazine, but its metabolites, might contribute to the beneficial effects of sulfasalazine.

Keywords: Disease-modifying antirheumatic drugs; B cells; Immunoglobulin; T cells; Anti-CD3

1. Introduction

Sulfasalazine has been used in the treatment of inflammatory bowel diseases (IBD) as well as rheumatic diseases, such as rheumatoid arthritis (RA) and ankylosing spondylitis [1–3]. Sulfasalazine consists of 5-aminosalicylic acid (5-ASA) and sulfapyridine (SP), linked by an azo bond. It remains unclear whether sulfasalazine itself or its metabolites are responsible for the antirheumatic effects, although a number of potential mechanisms of action of sulfasalazine and its metabolites have been proposed. Thus, sulfasalazine and 5-ASA inhibit cyclooxygenase [4] and 5-lipoxygenase [5]. Sulfasalazine and SP, but not 5-ASA, have been also shown to inhibit Ag-stimulated TNF-α production by mast cells [6]. Other studies showed that sulfasalazine, but not 5-ASA and SP, is anti-inflammatory in the murine air pouch model of inflammation [7].

* Corresponding author. Tel.: +81-3-3964-1211 Expt. 1568; fax: +81-3-3964-7094.

E-mail address: shunsei@med.teikyo-u.ac.jp (S. Hirohata).

1567-5769/02/$ - see front matter
PII: S1567-5769(01)00186-2

RA is characterized by chronic inflammation of synovial tissues in which immunologic abnormalities have been implicated [7,8]. One of the characteristic features of RA is chronic stimulation of B cells, as evidenced by the expression of rheumatoid factors as well as the collection of plasma cells in the synovium [8,9]. In fact, most of disease-modifying antirheumatic drugs (DMARDs) have been shown to suppress the in vitro Ig production at their pharmacologically relevant concentrations [10,11]. A previous report disclosed that relatively higher concentrations of sulfasalazine and 5-ASA (more than 0.1 mM) inhibited pokeweed mitogen-stimulated Ig production [12]. However, since pokeweed mitogen-stimulated Ig production is totally dependent on T cells [13], it is not clear whether sulfasalazine and 5-ASA directly suppress B cells. The current studies were therefore undertaken to explore the effects of sulfasalazine and its metabolites on the functions of T cells and B cells at their pharmacologically relevant concentrations.

2. Materials and methods

2.1. Reagents

Several MAbs were used in the current studies, including 64.1, a murine IgG2a MAb directed to the CD3 complex on mature T cells (a gift of Dr. Peter E. Lipsky, NIAMS, Bethesda, MD), B9.11, a murine IgG1 MAb directed to the human CD8 molecule (Immunotech, Marseille, France) and IOT2a (Immunotech), an IgG2b MAb directed at monomorphic HLA-DR determinants. Phycoerythrin (PE)-conjugated anti-IL-2R1 (CD25) MAb (murine IgG2a; Coulter, Miami, FL) and PE-conjugated control murine IgG2a (Dako, Glostrup, Denmark) were used for immunofluoresent staining. Formalinized Cowan I strain *Staphylococcus aureus* (SA) was purchased from Calbiochem-Behring (San Diego, CA) and was used at a concentration of 1/240,000 (v/v). Recombinant human IL-2 (TGP-3) was a gift of Takeda Chemical Industries (Osaka, Japan); unit activity was determined by the provider (4.2×10^4 units/mg protein). Sulfasalazine, SP, 4-acetyl-SP, and 5-ASA were synthesized and were provided by Santen Pharmaceutical (Osaka, Japan).

2.2. Culture medium

RPMI 1640 medium (Life Technologies, Grand Island, NY) supplemented with penicillin G (100 unit/ml), streptomycin (100 μg/ml), L-glutamine (0.3 mg/ml), and 10% fetal bovine serum (Life Technologies) was used for all cultures.

2.3. Cell preparation

PBMC were obtained from healthy adult volunteers by centrifugation of heparinized venous blood over sodium diatrizoate-Ficoll gradient (Histopaque; Sigma, St. Louis, MO), and are depleted of monocytes and NK cells by incubation with 5 mM L-leucine methyl ester HCl (Sigma) in serum-free RPMI 1640, as described elsewhere [14]. The treated cell population was washed twice and then incubated with neuraminidase-treated sheep red blood cells (*N*-SRBC). The rosetting and nonrosetting populations were then separated by centrifugation on sodium diatrizoate-Ficoll gradients. The nonrosetting cells obtained from the interface were again rosetted with *N*-SRBC and centrifuged on sodium diatrizoate-Ficoll gradients to remove residual T cells. The resultant population of B cells contained <1% CD14+ monocytes and <1% CD2+CD3+ T cells, as determined by analysis with flow cytometry. The cells were additionally characterized as containing >90% CD20+ B cells and no CD16+ NK cells. The sedimented *N*-SRBC rosette-forming cells from the first centrifugation were treated with isotonic NH_4Cl to lyse the *N*-SRBC and were then passed over a nylon-wool column. The resultant population of T cells contained <0.1% esterase-positive monocytes and <0.5% CD20+ B cells.

Purified CD4+ T cells were prepared from the total T cell population by negative selection, using a panning technique to deplete contaminating HLA-DR+ cells and CD8+ T cells, as previously indicated [15]. The CD4+ T cell population obtained in this manner contained <2% CD8+ T cells and >96% CD4+ T cells.

2.4. Cell culture techniques for induction of immunoglobulin production

B cells ($2.5-5.0\times10^4$/well) were cultured alone in wells of 96-well U-bottom microtiter plates (No.3799,

Costar, Cambridge, MA) with SA+IL-2 (0.1 unit/ml). Cultures were carried out in duplicate or triplicate in a total volume of 200 μl. The cells were incubated for 10 days at 37 °C in a humidified atmosphere of 5% CO_2 and 95% air.

2.5. Measurement of IgM and IgG

Microtiter plates (Dynex, Chantilly, VA) coated with $F(ab')_2$ fragments of goat anti-human IgM or anti-human IgG (Cappel Laboratories, West Chester, PA) were incubated with cell-free culture supernatants or IgM or IgG standards in PBS containing 1% bovine serum albumin (Miles, Elkhart, IN). Bound IgM or IgG was detected with peroxidase-conjugated $F(ab')_2$ fragments of goat anti-human IgM or IgG (Cappel) as previously described [16].

2.6. Culture techniques for induction of T cell proliferation and IFN-γ production

MAb 64.1 was diluted in RPMI 1640 (2 μg/ml), and 50 μl was placed in each well of 96-well flat-bottom microtiter plates (No. 3596, Costar) and incubated at room temperature for 1 h. The wells were then washed once with culture medium to remove

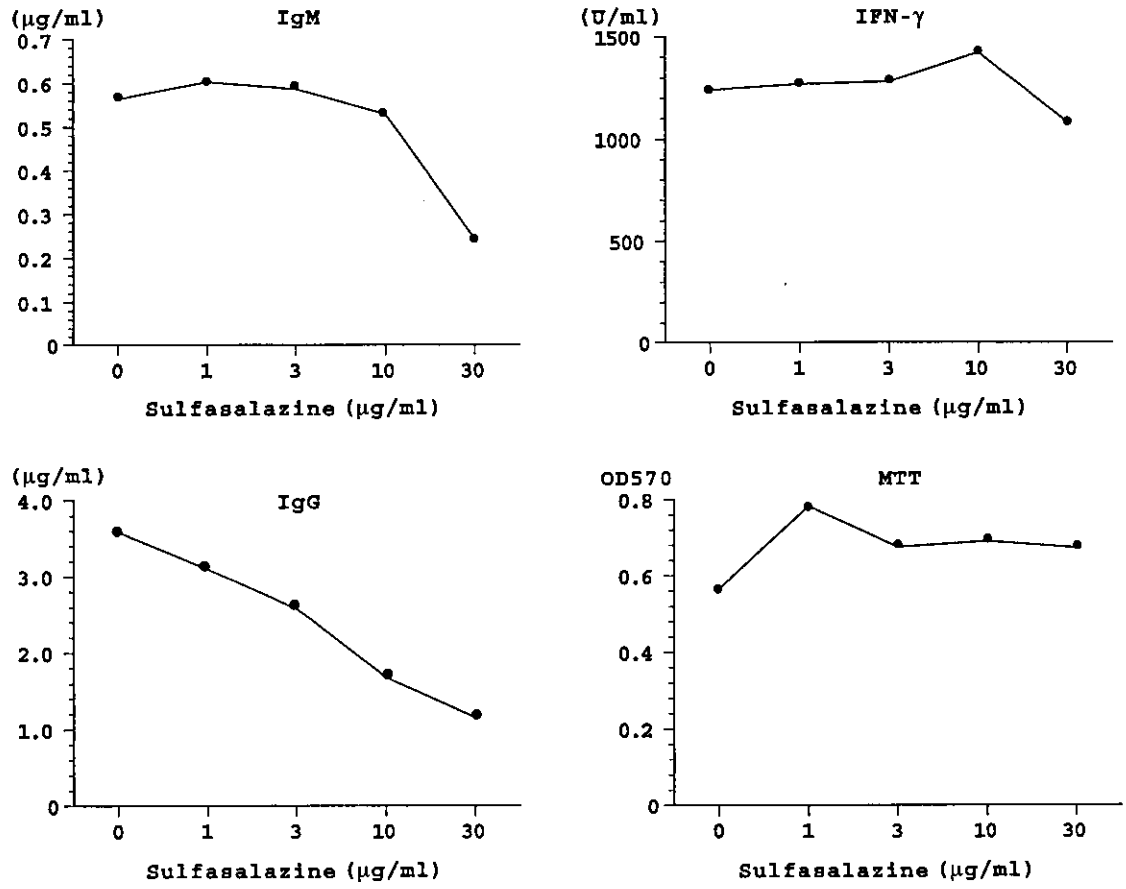

Fig. 1. The effects of sulfasalazine on B cell production of IgM and IgG and on T cell proliferation and IFN-γ production. B cells (2.5×10^4/well) were cultured with SA+IL-2 (0.1 unit/ml) for 10 days. CD4+ T cells (2×10^5 /well) were cultured in wells with immobilized anti-CD3 (64.1, 100 ng/well) for 5 days. Various concentrations of sulfasalazine were added as indicated. After incubation, T cell proliferation was assessed by the colorimetric assay as described in Materials and methods. The supernatants in B cell cultures or in T cell cultures were harvested and assayed for IgM and IgG content or for IFN-γ, respectively, by enzyme-linked immunosorbent assay (ELISA).

non-adherent MAb before the cells were added. Approximately 14–20% of the added MAb adhered to the wells [14,15]. Cultures were carried out in triplicate in a total volume of 200 μl. CD4+ T cells ($1-2\times10^5$/well) were cultured in wells with immobilized anti-CD3 for 5 days. After the incubation, the supernatants were harvested for the assay of IFN-γ contents, and the proliferation of T cells was assessed by an MTT cell growth assay kit (Chemicon, El Segundo, CA) [17]. IFN-γ contents in the supernatants were measured using a solid-phase enzyme immunoassay as previously described [18]. Previous studies revealed that the proliferation and IFN-γ production of T cells stimulated with immobilized anti-CD3 (64.1) reached the maximal level after 5 days from the initiation of the cultures [19].

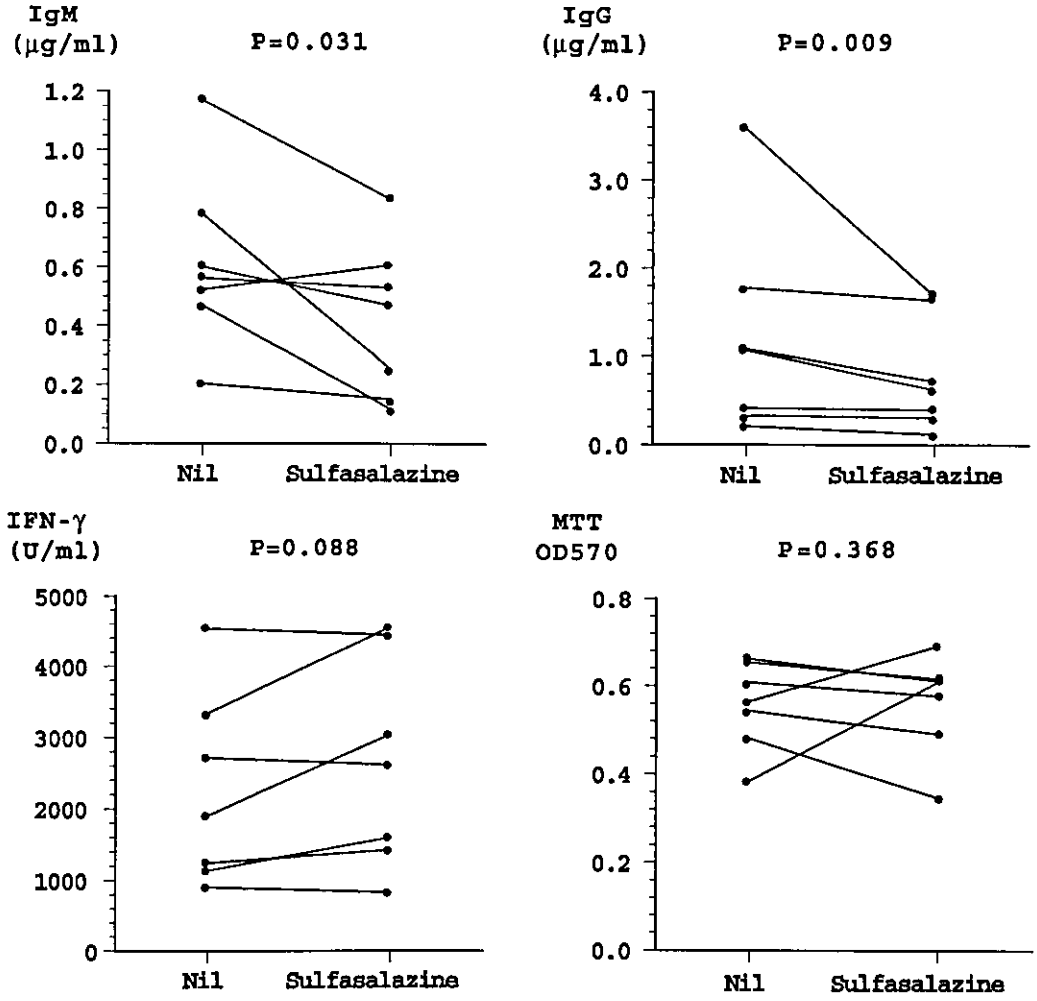

Fig. 2. Comparison of the effects of sulfasalazine on B cell production of IgM and IgG and on T cell proliferation and IFN-γ production. B cells (2.5×10^4/well) were cultured with SA+IL-2 (0.1 unit/ml) for 10 days. CD4+ T cells ($1-2\times10^5$ /well) were cultured in wells with immobilized anti-CD3 (64.1, 100 ng/well) for 5 days. Sulfasalazine were added as indicated. After incubation, T cell proliferation was assessed by the colorimetric assay as described in Materials and methods. The supernatants in B cell cultures or in T cell cultures were harvested and assayed for IgM and IgG content or for IFN-γ, respectively, by ELISA. The significance of the effects of sulfasalazine in seven different individuals was evaluated by Wilcoxon's signed rank test.

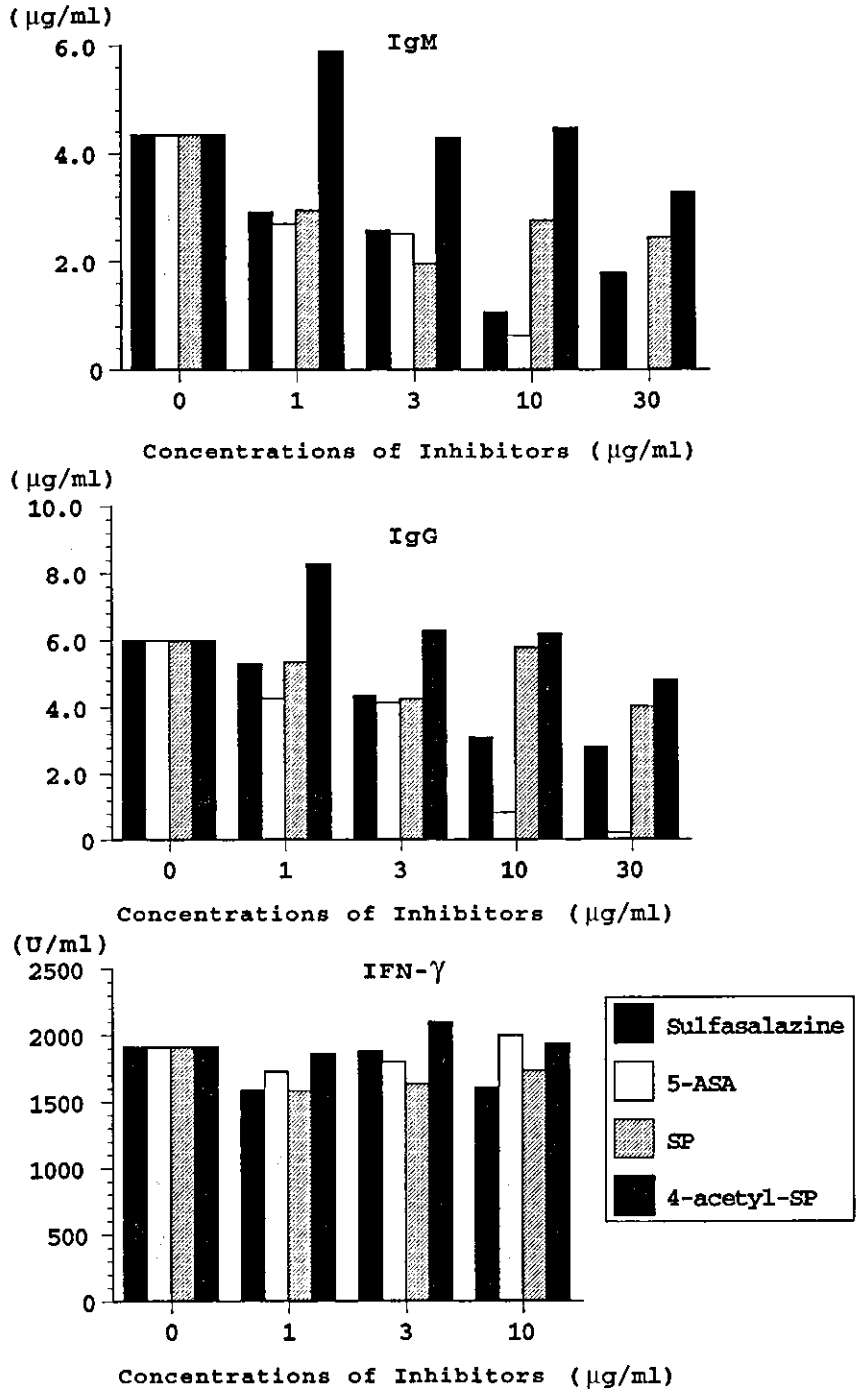

Fig. 3. Comparison of the effects of sulfasalazine and its metabolites on B cell production of IgM and IgG and on IFN-γ production of CD4+ T cells. B cells (2.5×10^4/well) were cultured with SA+IL-2 (0.1 unit/ml) for 10 days. CD4+ T cells (2×10^5/well) were cultured in wells with immobilized anti-CD3 (64.1, 100 ng/well) for 5 days. Sulfasalazine and its metabolites were added as indicated. After incubation, the supernatants in B cell cultures or in T cell cultures were harvested and assayed for IgM and IgG content or for IFN-γ, respectively, by ELISA.

2.7. Immunofluorescent staining and analysis

SA-stimulated B cells ($4-10\times10^5$/sample) were stained with PE-conjugated anti-CD25 MAb or control MAb. Briefly, after washing with 2% normal goat serum in PBS and 0.1% sodium azide (staining buffer), cells were stained with PE-conjugated anti-CD25 MAb or control murine IgG2a MAb for 30 min. The cells were then washed three times with staining buffer, and were fixed with 1% paraformaldehyde for 5 min at room temperature. The cells were then analyzed using an EPICS XL flow cytometer (Coulter, Hialeah, FL) equipped with an argon–ion laser at 488 nm. A gating on the forward and side scatter measurement was used to identify viable lymphocytes. The percentages of cells that were stained positively for anti-CD25 were determined by integration of cells above a specific fluorescence channel, calculated in relation to the staining with control IgG2a MAb.

2.8. Statistical analysis

The statistical significance of the effects of sulfasalazine and its metabolites on the T cell proliferation

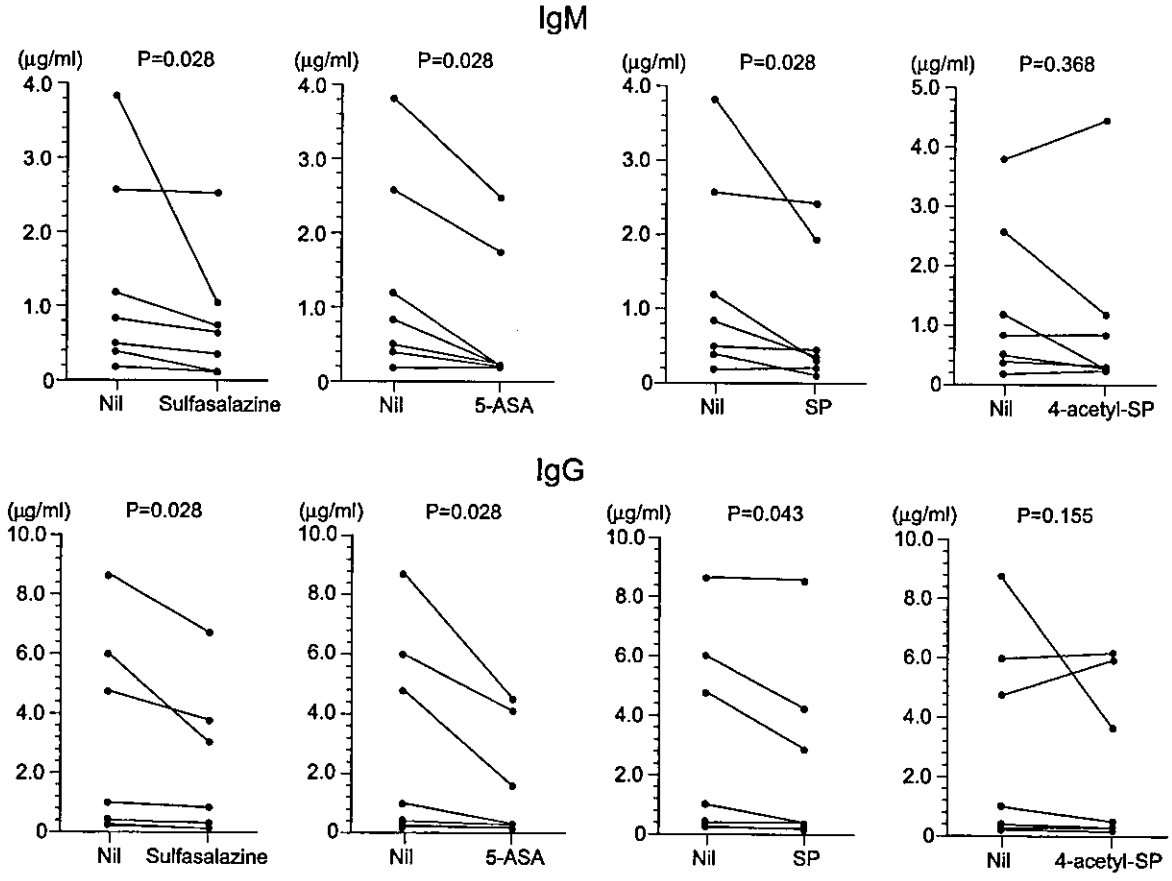

Fig. 4. Comparison of the effects of sulfasalazine and its metabolites on B cell production of IgM and IgG and on IFN-γ production of CD4+ T cells. B cells (2.5×10^4/well) were cultured with SA+IL-2 (0.1 unit/ml) for 10 days. CD4+ T cells ($1-2\times10^5$/well) were cultured in wells with immobilized anti-CD3 (64.1, 100 ng/well) for 5 days. Sulfasalazine (10 μg/ml), 5-ASA (3 μg/ml), SP (3 μg/ml), and 4-acetyl-SP (10 μg/ml) were added as indicated. After incubation, the supernatants in B cell cultures or in T cell cultures were harvested and assayed for IgM and IgG content or for IFN-γ, respectively, by ELISA. The significance of the effects of sulfasalazine and its metabolites in seven different individuals was evaluated by Wilcoxon's signed rank test.

and IFN-γ production and on the B cell production of IgM and IgG in different individuals was evaluated by Wilcoxon's signed rank test.

3. Results

3.1. Differential suppressive effects of sulfasalazine on the functions of T cells and B cells

Initial experiments explored the influences of various concentrations of sulfasalazine on the production of IgM and IgG by B cells and on the proliferation and IFN-γ production of T cells. The production of IgM and IgG was induced from highly purified B cells by stimulation with SA+IL-2. T cell proliferation and IFN-γ production were induced by stimulation with immobilized anti-CD3 in the complete absence of monocytes [15]. As can be seen in Fig. 1, sulfasalazine suppressed the production of IgM and IgG by SA-stimulated B cells in a dose-dependent manner. By contrast, sulfasalazine did not suppress the proliferative responses and IFN-γ production of immobilized anti-CD3 stimulated CD4+ T cells at concentrations of 1–30 μg/ml. Moreover, as shown in Fig. 2, sulfasalazine at its pharmacologically attainable concentration of 10 μg/ml (25 μM) significantly suppressed the production of IgM and IgG induced by SA+IL-2, whereas it did not

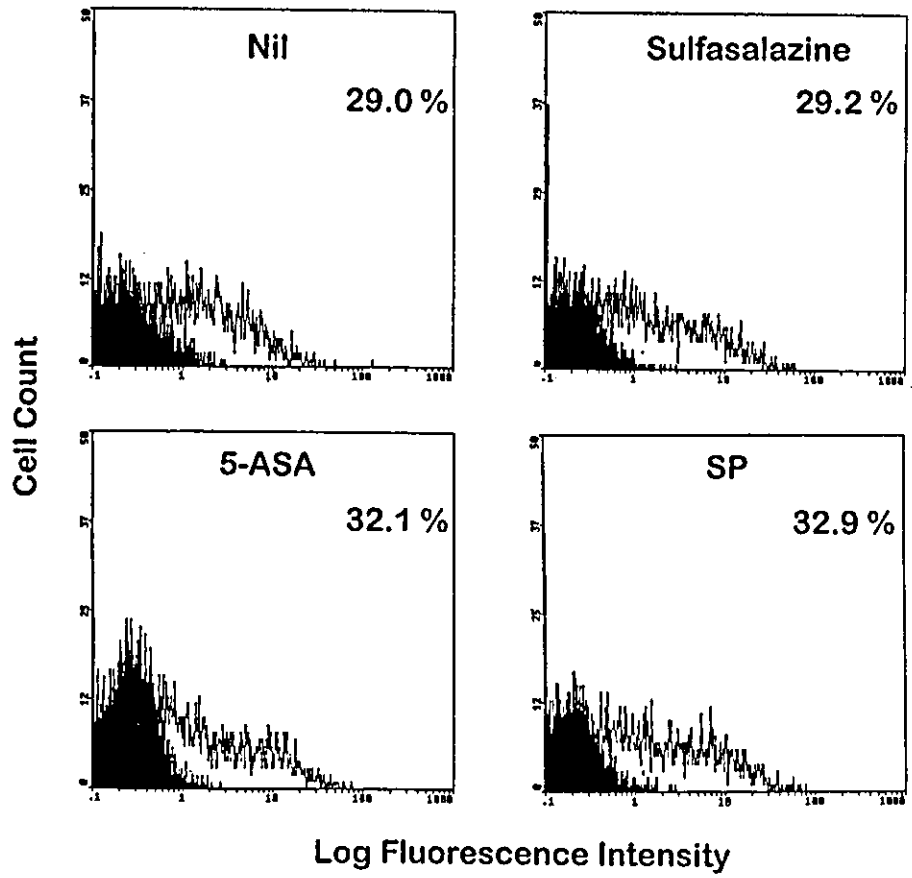

Fig. 5. Neither sulfasalazine nor its metabolites suppress the expression of IL-2 receptor (CD25) on SA-activated B cells. B cells were cultured with SA+IL-2 (0.1 unit/ml) in the presence or the absence of sulfasalazine (25 μM), SP (40 μM) or 5-ASA (60 μM). After 24 h of culture, the cells were harvested and stained with PE-conjugated anti-CD25 MAb (IgG2a) or control IgG2a MAb, and then were analyzed by flow cytometry. The percentages of cells positive for CD25 are shown.

suppress the IFN-γ production and proliferation of immobilized anti-CD3 stimulated CD4+ T cells in seven healthy individuals. These results indicate that at pharmacologically attainable concentrations, sulfasalazine selectively suppresses B cells responses, but not T cell responses.

3.2. Differential effects of sulfasalazine and its metabolites on the functions of T cells and B cells

Next experiments were undertaken to compare the effects of sulfasalazine and its major metabolites on the function of T cells and B cells. As can be seen in Fig. 3, any of sulfasalazine and its metabolites, including 5-ASA, SP, and 4-acetyl-SP, did not inhibit the IFN-γ production of immobilized anti-CD3-stimulated CD4+ T cells. By contrast, sulfasalazine as well as its metabolites 5-ASA and SP suppressed the production of IgM and IgG at concentrations of 1–30 μg/ml, whereas 4-acetyl-SP did not suppress the production of IgM and IgG at any concentrations. To confirm that sulfasalazine and its metabolites, 5-ASA and SP, inhibit in vitro B cell functions, experiments were designed to compare the effects of sulfasalazine and its metabolites to suppress the production of IgM and IgG by SA-stimulated B cells at their pharmacologically attainable concentrations. B cells from seven healthy individuals were cultured with SA+IL-2 in the presence absence of sulfasalazine (25 μM; 10 μg/ml) and its metabolites, including 5-ASA (20 μM; 3 μg/ml), SP (12 μM; 3 μg/ml), and 4-acetyl-SP (35 μM; 10 μg/ml). After 10 days of incubation, the supernatants were harvested and assayed for IgM and IgG contents. As can be seen in Fig. 4, sulfasalazine as well as 5-ASA and SP, but not 4-acetyl-SP, significantly suppressed the production of IgM and IgG at their pharmacologically attainable concentrations [20,21], whereas none of them inhibited the IFN-γ production of anti-CD3-stimulated CD4+ T cells. The results therefore indicate that sulfasalazine and its metabolites, 5-ASA and SP, specifically suppress the function of B cells, but not that of T cells.

3.3. The effects sulfasalazine and its metabolites on the CD25 expression of B cells

To explore the stages of B cell activation in which sulfasalazine and its metabolites exert its suppressive effects, final experiments were designed in which the influence of sulfasalazine, SP and 5-ASA on the expression of CD25 was assessed by flow cytometry. As shown in Fig. 5, none of sulfasalazine, SP and 5-ASA inhibited the expression of CD25 on B cells stimulated with SA+IL-2 for 24 h. The results indicate that neither sulfasalazine nor its metabolites inhibit the early events in B cell activation. It is thus suggested that sulfasalazine and its metabolites might suppress the events involved in the cell cycle after the G1 phase.

4. Discussion

Previous studies have reported that relatively high concentrations of sulfasalazine and 5-ASA (0.1 mM), but not SP, inhibited pokeweed mitogen-stimulated Ig production [12]. However, since pokeweed mitogen-stimulated Ig production is totally dependent on T cells [13], it remained unclear whether sulfasalazine and 5-ASA directly suppress B cells. Nor has it been clear whether SP could suppress B cell responses. The results in the current studies using SA-stimulated B cells clearly demonstrate that sulfasalazine as well as its metabolites, 5-ASA and SP, inhibit the production of IgM and IgG of human B cells at their pharmacologically relevant concentrations (1–10 μg/ml) [20, 21]. These results therefore suggest that at least one of the mechanisms of action of sulfasalazine in RA as well as IBD might involve the suppression of B cells.

The results in the present study also revealed that at pharmacologically attainable concentrations any of sulfasalazine and its metabolites did not suppress the IFN-γ production of immobilized anti-CD3-stimulated CD4+ T cells. Of note, it has been also shown that T cells also play an important role in the pathogenesis of RA. It is therefore suggested that combined use of cyclosporin A [22], which suppresses the function of T cells, with sulfasalazine might enhance the beneficial effects in the treatment of RA.

The beneficial effects of 5-ASA (mesalazine) in the treatment of IBD, such as ulcerative colitis and Crohn's disease, have been well appreciated [1]. It has been shown that abnormal B cell functions are involved in the pathogenesis of IBD. Thus, the intestines of IBD contained higher numbers of Ig-producing cells [23, 24]. Moreover, it has been also disclosed that major alterations in the synthesis and secretion patterns of Ig

occur with IBD peripheral blood and intestinal mononuclear cells [25–27]. Therefore, the results in the current studies suggest that sulfasalazine and mesalazine might play a role in the treatment of IBD by directly inhibiting the function of B cells in the systemic circulation as well as in the intestine.

Previous studies suggested that the active moiety for IBD seemed to be 5-ASA [28], but is SP for RA [29]. Of note, it has been shown that one of the characteristic features of RA is chronic stimulation of B cells, as evidenced by the expression of rheumatoid factors as well as the collection of plasma cells and the formation of lymphoid follicles in the synovium [8,9]. Although the plasma concentration of 5-ASA is <7 μM after administration of sulfasalazine, it can be elevated by direct administration of 5-ASA or its controlled-release formulation (mesalazine) [21]. Since 5-ASA (20 μM) suppressed the B cell responses as effectively as sulfasalazine (25 μM) at pharmacologically attainable concentrations, it is suggested that mesalazine might also have beneficial effects in the treatment of RA. However, a number of clinical studies demonstrated that 5-ASA was ineffective in the treatment of RA, whereas SP was as effective as sulfasalazine [29,30]. This was not due to the low concentrations of 5-ASA in the plasma [29]. It should be noted that 5-ASA is rapidly acetylated after absorption to form *N*-acetyl 5-ASA, which is biologically inactive [31,32]. Therefore, it is likely that the instability of 5-ASA in the plasma might result in the incomplete interaction with B cells. By contrast, mesalazine is a controlled-release formulation of 5-ASA, which enable 5-ASA to stay all over the intestine in its native form [21], thus accounting for its efficacy in IBD through interactions with B cells infiltrated in the intestines. On the other hand, the results in the current studies disclosed that sulfasalazine inhibited the function of B cells as effectively as SP, which is consistent with the results of the previous clinical studies that SP was as effective as sulfasalazine for RA [29,30]. Thus, it is most likely that both of sulfasalazine and SP might be the active moiety of sulfasalazine in RA.

The results in the current studies could not identify the precise mechanisms of action of sulfasalazine and its metabolites, 5-ASA and SP, in the suppression of human B cell responses. However, the data disclosed that none of sulfasalazine, SP and 5-ASA suppressed the expression of CD25 on SA-stimulated B cells. Thus, it is clear that sulfasalazine and its metabolites do not inhibit the initial stages of B cell activation. In this regard, the suppressive effects of sulfasalazine and its metabolites are different from those of gold compounds, which have been shown to inhibit the initial activation of B cells [10]. The data therefore suggest the efficacy of a combination of sulfasalazine with such DMARDs that inhibit the initial activation of B cells, including gold compounds.

Acknowledgements

This work was supported by 2001 grant (C2) 12670438 from the Ministry of Education, Culture, Science and Sports of the Japanese Government and by grants from Santen Pharmaceutical, Osaka, Japan, and from Manabe Medical Foundation, Tokyo, Japan. The authors wish to thank Chise Kawashima for preparing the manuscript and the illustrations.

References

[1] Klotz U, Maier K, Fischer C, Heinkel K. Therapeutic efficacy of sulfasalazine and its metabolites in patients with ulcerative colitis and Crohn's disease. N Engl J Med 1980;303:1499–502.

[2] Bax DE, Greaves MS, Amos RS. Sulfasalazine for rheumatoid arthritis: relationship between dose, acetylator phenotype, and response to treatment. Br J Rheumatol 1986;25:282–4.

[3] Dougados M, Boumier P, Amor B. Sulphasalazine in ankylosing spondylitis: a double-blind controlled study in 60 patients. Br Med J 1986;293:911–4.

[4] Hawkey CJ, Truelove SC. Inhibition of prostaglandin synthetase in human rectal mucosa. Gut 1983;24:213–7.

[5] Stenson WF, Lobos E. Sulfasalazine inhibits the synthesis of chemotactic lipids by neutrophils. J Clin Invest 1982;69:494–7.

[6] Bissonnette EY, Enciso JA, Befus AD. Inhibitory effects of sulfasalazine and its metabolites on histamine release and TNF-α production by mast cells. J Immunol 1996;156:218–23.

[7] Gadangi P, Longaker M, Naime D, Levin RI, Recht PA, et al. The anti-inflammatory mechanism of sulfasalazine is related to adenosine release at inflamed sites. J Immunol 1996;156:1937–41.

[8] Wernick RM, Lipsky PE, Marban-Acos E, Maliakkal JJ, Edelbaum D, et al. IgG and IgM rheumatoid factor synthesis in rheumatoid synovial membrane cell cultures. Arthritis Rheum 1985;28:742–52.

[9] Dechanet J, Merville P, Durand I, Banchereau J, Miossec P. The ability of synoviocytes to support terminal differentiation

A．総論—Ⅲ．リウマチ性疾患の臓器病変の把握と考え方

リウマチ性疾患の精神・神経病変*

広畑俊成**

Key words: Systemic lupus erythematosus, Behçet's disease, Rheumatoid arthritis, Cerebrospinal fluid, IL-6

はじめに

各種のリウマチ性疾患においては多彩な神経病変がみられる．中でも，とくに全身性エリテマトーデス(SLE)やベーチェット病においては，中枢神経病変は主要な症状の1つであり，CNSループスあるいは神経ベーチェット症候群(NB)とよばれている．これらの発症機序については不明な点が多く，また診断にも苦慮することが少なくなかった．しかし，近年，とくに髄液の免疫グロブリン・サイトカインの異常と各種炎症性中枢神経疾患の関係が注目されてきており[1]，CNSループスやNBにおいても，その発症にあたって中枢神経内の免疫異常が重要な役割を果たすことが明らかになってきている．一方，こうした中枢神経症状とは別に，とくに慢性関節リウマチなどにおいては末梢神経障害を生じることがある．本稿においては，CNSループスおよびNBを中心として，中枢神経内の免疫異常と病態とのかかわりについて概説するとともに，慢性関節リウマチによる神経症状についても触れてみたい．

SLEの中枢神経症状(CNSループス)

1．臨床的特徴

SLEそのものに起因すると考えられる精神神経症状は，表1に示すように実に多彩なものである．この中でとくに頻度の高いものが，高次脳機能の異常(広義の精神症状)とけいれんである．高次脳機能の異常は，見当識・記憶・認知・計算などの知的機能の異常を主徴とする脳器質症候群(organic brain syndrome)と，神経症・抑うつ・精神分裂病様症状などの精神症状を主体とする非器質性精神病(non-organic psychosis)に大別される[2]．実際には，この両者の混在する場合もみられる．また，こうした精神症状が重篤になると，高度の意識障害(ときに昏睡状態)をきたしたりけいれんの重積発作を併発したりすることがある．一方，高次脳機能の異常がまったくない患者にけいれん・意識消失発作などが単独でみられる場合も少なくない．片マヒなどの局所神経徴候は，抗リン脂質抗体症候群に起因する場合が多い．無踏病などの不随意運動は稀であるがSLEに比較的特異的な合併症である．注意しなくてはならないのは，SLEの増悪に際して副腎皮質ステロイドを増量した後に精神症状が出現したり増悪したりすることがある点である．これは単純な副腎皮質ステロイドの副作用(いわゆるsteroid psychosis)ではなく，むしろ潜在的に進行していたCNSループスが副腎皮質ステロイドの投与によって一気に顕在化したと考えるべきである．事実，このような場合はステロイドの維持もしくは増量により改善することが多い．一方，以前より副腎皮質ステロイドによる

* Neuropsychiatric manifestations in rheumatic diseases.

** Shunsei HIROHATA, M.D.: 帝京大学医学部内科〔〒173-8605 東京都板橋区加賀2-11-1〕; Department of Internal Medicine, Teikyo University School of Medicine, Tokyo 173-8605, JAPAN